Monomeric and Dimeric Iron(III) Complexes of 5-Hydroxy-10,15,20-triphenylporphyrin: Formation of Cyano and Pyridine Complexes of (5-Oxo-10,15,20-triphenylphlorin)iron

Jacek Wojaczyński,[a] Marcin Stępień,[a] and Lechosław Latos-Grażyński*[a]

Keywords: Porphyrinoids / Oxophlorins / Iron / Electronic structure / NMR spectroscopy

The reaction of $[(TrPP)Fe^{II}(py)_2]$ (TrPP = dianion of 5,10,15-triphenylporphyrin) with hydrogen peroxide results in oxygenation of the (porphyrin)iron and the formation of (10,15,20-triphenyl-5-oxophlorin)iron $[(5\text{-}O\text{-}TrPP)Fe(py)_2]$. Coupled oxidation of $[(TrPP)Fe^{III}Cl]$ in the presence of ascorbic acid and potassium cyanide in methanol leads to oxidative hydroxylation of the porphyrin ring to form a cyclic dimer $[(5\text{-}O\text{-}TrPP)Fe^{III}]_2$. Three out of four pyrrole ^{1}H NMR resonances of the dimeric complex present the characteristic displacement with respect to the typical position for the high-spin (tetraphenylporphyrin)iron(III) complexes. The linewidths of the β-H pyrrole resonances correlate with specific locations of the respective protons within the dimeric structure. Addition of HCl to $[(5\text{-}O\text{-}TrPP)Fe^{III}]_2$ results in cleavage of the dimer producing $[(5\text{-}OH\text{-}TrPP)Fe^{III}Cl]$. $[(5\text{-}O\text{-}TrPP)Fe^{III}]_2$ is also split with acetic anhydride to give (5-acetoxy-10,15,20-triphenylporphyrin)iron(III). In the presence of $[D_5]$pyridine or a large excess of cyanide ion, $[(5\text{-}O\text{-}TrPP)Fe^{III}]_2$ undergoes cleavage to form air-sensitive $[(5\text{-}O\text{-}TrPP)Fe(py)_2]$ or $[(5\text{-}O\text{-}TrPP)Fe(CN)_2]^{2-}$. The pyrrole pattern observed for $[(5\text{-}O\text{-}TrPP)Fe(py)_2]$ is similar to that determined on the basis of an analysis carried out for four (oxophlorin)-iron regioisomers obtained from hemes. For comparison, the characteristic ^{1}H NMR features of the typical (5-substituted-10,15,20-triphenylporphyrin)iron(III) complexes have been investigated for the series of high-spin and low-spin complexes. The spin-density distribution in the (oxophlorin)iron skeleton is dominated by the radical-like electronic structure.

Introduction

Coordinating properties of porphyrins, widely used in biomimetic chemistry and catalytic studies, can be remarkably modified by the introduction of some additional metal ion coordinating centers at the porphyrin periphery. Such substituents are suitable for coordination of the metal ion of the same or other molecular systems.[1−3] These ''hybrid'' bifunctional ligands combine properties of the porphyrin macrocycles with those of the peripheral coordinating moiety.

The hydroxy-substituted octaethylporphyrin and tetraphenylporphyrin are representative examples of polyfunctional ligands related to porphyrins. They are able to coordinate through the tetranitrogen macrocyclic center and/or through an ionized hydroxy group at the periphery. Three structurally distinct locations of the hydroxy substituents for the originally highly symmetrical model porphyrins $OEPH_2$ and $TPPH_2$ were attainable synthetically, a *meso* position for $OEPH_2$, and β-pyrrole or phenyl positions for $TPPH_2$.[4−7] Insertion of an iron ion into 5-(2-hydroxyphenyl)-10,15,20-tritolylporphyrin ($TTOPH_2$) or 5-hydroxy-octaethylporphyrin (octaethyloxophlorin, $OEPOH_2$) resulted in the formation of the high-spin doubly oxo-bridged iron(III) head-to-tail dimers $[(TTOP)Fe^{III}]_2$ and $[(OEPO)Fe^{III}]_2$, respectively.[8−10] Dimerization through phenoxide $\{[(TTOP)Fe^{III}]_2\}$ or the *meso*-oxygen atom $\{[(OEPO)Fe^{III}]_2\}$ rather than μ-oxo bridging was preferred in both cases.

The structure of $[(TTOP)Fe^{III}]_2$ was determined by X-ray crystallography and the retention of the dimeric structure in solution was demonstrated by ^{1}H NMR spectroscopy.[8,9] Goff et al. characterized the manganese(III) dimer $[(TTOP)Mn^{III}]_2$ and detected, by means of ^{1}H NMR spectroscopy, the diphenoxo-bridged heteronuclear complex $[(TTOP)Fe^{III}(TTOP)Mn^{III}]$.[9]

(Oxophlorin)iron complexes are significant in the context of their involvement as intermediates in the conversion of (porphyrin)iron to biliverdin in the oxidative heme destruction.[11,12] Masuoka and Itano characterized the (oxophlorin)iron(III) dimer $[(OEPO)Fe^{III}]_2$ by a range of spectroscopic techniques.[10] The presence of two paramagnetic centers produced marked changes of the ^{1}H NMR spectral parameters compared to monomeric analogs, including variation of the linewidths for the methylene protons.[13] The formation of $[(OEPO)Mn^{III}]_2$ has been demonstrated,[14] and the unique structure of the related indium complex determined by X-ray crystallography.[15]

[a] Department of Chemistry, University of Wrocław,
14 F. Joliot-Curie St., 50-383 Wrocław, Poland
E-mail: llg@wchuwr.chem.uni.wroc.pl

2-Hydroxy-5,10,15,20-tetraphenylporphyrin is the tetraphenylporphyrin derivative hydroxylated at a β-position. The cyclic trimers $[(2\text{-O-TPP})Fe^{III}]_3$, $[(2\text{-O-TPP})Ga^{III}]_3$, and $[(2\text{-O-TPP})Mn^{III}]_3$ were generated in a self-assembly process of monomeric (2-hydroxy-5,10,15,20-tetraphenylporphyrin)iron(III), -gallium(III), or -manganese(III).[16−18] The trivalent metal ion coordinated in the porphyrin crevice seems to be a prerequisite for the trimer formation. The paramagnetic heterometallic head-to-tail cyclic trimers of general formula $[(2\text{-O-TPP})M^{III}]_n[(2\text{-O-TPP})M_1^{III}]_{3-n}$ (M, M_1: Fe^{III}, Ga^{III}, Mn^{III}) have also been identified.[19]

In this project we introduce a new hybrid bifunctional ligand, namely 5-hydroxy-10,15,20-triphenylporphyrin (5-OH-$TrPPH_2$) which is formally derived from tetraphenylporphyrin. The molecule is "constructed" by replacement of a single *meso*-phenyl group with a hydroxy group.

5-OH-$TrPPH_2$ and the previously investigated 5-hydroxyoctaethylporphyrin contain the identical structural motif of 5-hydroxyporphyrin.[20] In analogy to 5-OH-$OEPH_2$, the coordinating properties of 5-OH-$TrPPH_2$ can be related to two tautomers, 5-hydroxyporphyrin and 5-oxophlorin, presented in Scheme 1.

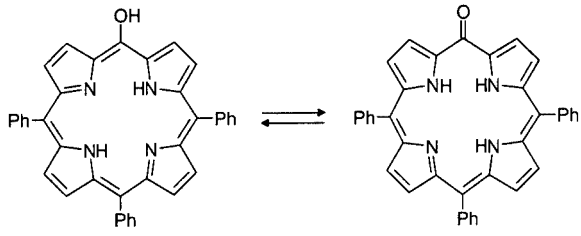

Scheme 1

In order to determine the influence of the *meso*-hydroxy group on (porphyrin)iron properties in a broader scope, a representative group of low-spin and high-spin iron(III) complexes of 5-substituted-10,15,20-triphenylporphyrin (5-X-$TrPPH_2$; X = NO_2, Br, *n*Bu, H, OMe) have been investigated in parallel. The 5-X substituents vary in their electron-donating/-withdrawing properties as measured by Hammett constants. Considering the biochemical aspects, the electronic structure and reactivity of the (5-oxo-10,15,20-triphenylphlorin)iron complex $[(5\text{-O-TrPP})FeL_2]$ (L = py, CN^-) are of particular interest.

The related (octaethyloxophlorin)Fe(pyridine)$_2$ complex {$[(OEPO)Fe(py)_2]$} has been studied extensively.[21−26] It has been found that a mechanism of coupled oxidation of $[(OEP)Fe^{II}(py)_2]$ in pyridine solution includes a *meso*-hydroxylation step producing $[(OEPO)Fe(py)_2]$.[12,27] It is widely accepted that the first step in heme degradation by heme oxygenase results in the *meso* hydroxylation of heme.[12,23,26,28,29] Direct spectroscopic evidence has been presented showing that *meso*-hydroxylated heme is formed by heme oxygenase.[30]

^{1}H NMR spectroscopy provides a uniquely useful probe for studying the structure of (porphyrin)iron complexes in solution.[31,32] The hyperfine shift patterns are particularly sensitive to the ligation, oxidation and spin state of the metal ion. For instance, the (porphyrin)iron(III) complexes bridged by ligands containing one or more oxygen atoms present ^{1}H NMR spectroscopic patterns unequivocally explainable in terms of their dimeric[8,9,13] or trimeric[16−19] structures. In this contribution our investigations have been focused on (5-hydroxy-10,15,20-triphenylporphyrin)- and (5-oxo-10,15,20-triphenylphlorin)iron(III) complexes. Four inequivalent pyrrole resonances of TrPP complexes and their *meso*-substituted derivatives provided the direct probe of the spin density around the porphyrin macrocycle, and allowed the detection of a cyclic dimeric structure.

Results and Discussion

Synthesis of [(5-X-TrPP)Fe^{III}Cl]

5,10,15-Triphenylporphyrin, $TrPPH_2$, was synthesized by the condensation of pyrrole, benzaldehyde, and paraformaldehyde. The procedure followed the methodology typically used for synthesis via a mixed aldehyde−pyrrole condensation.[33] Alternatively, $TrPPH_2$ was obtained by phenylation of 5,15-diphenylporphyrin with phenyllithium.[34]

$TrPPH_2$ was characterized by X-ray crystallography (Figure 1); the bond lengths and angles are within the range expected for a porphyrin.[35] The porphyrin macrocycle is practically flat. In the crystal, a 2_1 axis (along the *c* direction) generates a ribbon of molecules (Figure 1), which demonstrate a characteristic set of close CH−π contacts (with CH−centroid distances of 2.58 and 3.05 Å) involving Ph(5)···Ph(10)···Ph(15) *meso*-phenyl rings from adjacent triphenylporphyrins. An analogous structural motif has been observed for $TPPH_2$-based porphyrin sponges.[36,37] The periphery of $TrPPH_2$ presents a blending of structural features that are typical for $TPPH_2$ and $OEPH_2$ as the 5-*meso* position and two pyrrole rings are exposed.

5-Bromo-10,15,20-triphenylporphyrin (5-Br-$TrPPH_2$) was obtained from the reaction of $TrPPH_2$ with *N*-bromosuccinimide as described previously.[38] 5-Nitro-10,15,20-triphenylporphyrin (5-NO_2-$TrPPH_2$) was obtained by nitration of triphenylporphyrin with $AgNO_2$ in the presence of I_2 by modification of the method applied for the nitration of 5,15-diphenylporphyrin.[39]

Reaction of $[(TrPP)Zn^{II}]$ with sodium methoxide in the presence of air yielded (5-methoxy-10,15,20-triphenylporphyrin)zinc(II), which was subsequently demetallated with acid to give 5-MeO-$TrPPH_2$.

Iron insertion into 5-X-$TrPPH_2$ produced the corresponding $[(5\text{-X-TrPP})Fe^{III}Cl]$ complexes. The $[(5\text{-Br-TrPP})Fe^{III}Cl]$ complex was characterized by X-ray crystallography (Figure 2). The iron ion is five-coordinate with bonds to the four pyrrole nitrogen atoms of nearly equal lengths [2.065(4), 2.065(4), 2.071(4), and 2.076(4) Å]. The metal ion lies 0.461(2) Å out of the mean plane of the macrocycle. The Fe−N distances and the displacement from the mean plane are characteristic of five-coordinate high-spin (S = 5/2) (porphyrin)iron(III) complexes.[40−42] The Fe−Cl distance is 2.209(2) Å, which is typical for chloro(porphyrin)iron(III) complexes.[40,41]

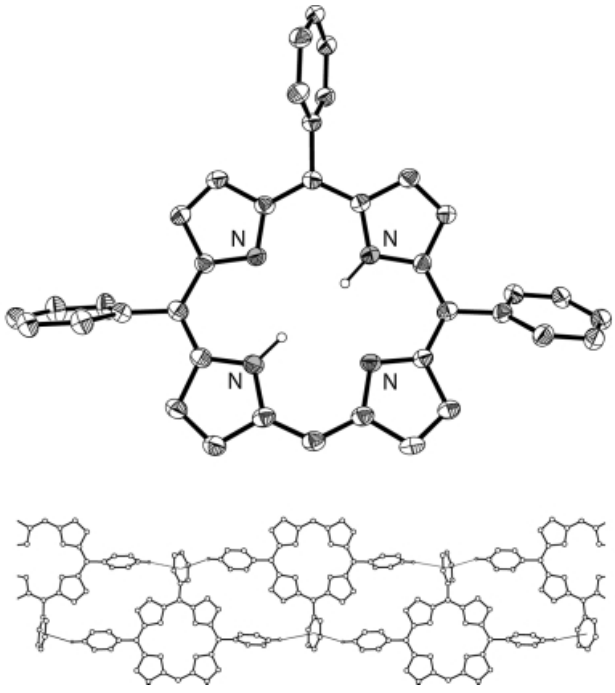

Figure 1. (top) The crystal structure of $TrPPH_2$; the vibrational ellipsoids represent 50% probability; (bottom) a view of the molecular packing demonstrating the ribbon arrangement and CH−π contacts of *meso*-phenyl rings from adjacent triphenylporphyrins

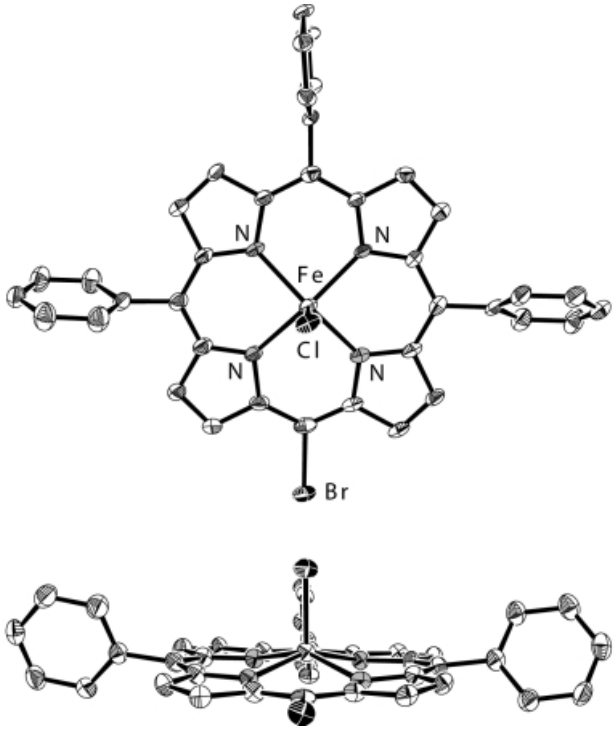

Figure 2. A perspective view of (5-Br-TrPP)$Fe^{III}Cl$ with 50% thermal contours

Reaction of Hydrogen Peroxide with [(TrPP)$Fe^{II}(py)_2$]

The standard hydroxylation procedure of $OEPH_2$ involves the reaction of [(OEP)Zn^{II}] with thallium(III) trifluoroacetate (TTFA) to produce (5-trifluoroacetoxyoctethylporphyrin)zinc(II) [(5-TFA-OEP)Zn^{II}].[4] Hydrolysis of this complex yields octaethyloxophlorin. Quite differently, the [(TrPP)Zn^{II}] complex undergoes a regiospecific C(5)−C(5′) coupling, mediated by TTFA acting solely as a two-electron oxidizing reagent to produce [5,5′-bi(10,15,20-triphenylporphyrin)]dizinc(II) [$(TrPP)_2Zn^{II}_2$].[43−45] Consequently, to obtain (5-hydroxy-10,15,20-triphenylporphyrin)iron(III), a different approach has been applied. We have taken into account that porphyrins themselves are not nearly as susceptible to initial *meso* oxygenation (hydroxylation) as are (porphyrin)iron complexes.[26,46,47] Consequently, the reaction of [(TrPP)$Fe^{II}(py)_2$] with hydrogen peroxide at −30 °C in the absence of dioxygen has been examined. Scheme 2 shows the structures and transformations involved.

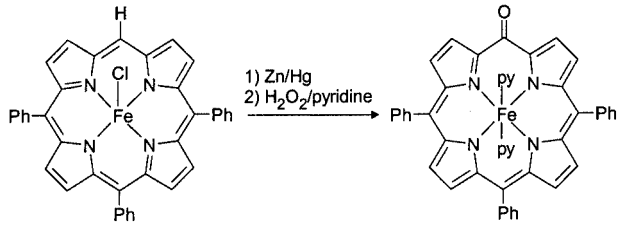

Scheme 2

A [D_5]pyridine solution of [(TrPP)$Fe^{II}(py)_2$] was prepared under dinitrogen to exclude any oxidation with dioxygen and cooled to −30 °C, at which point a dioxygen-free solution of hydrogen peroxide (30% in water)/[D_5]pyridine solution (1:60, v/v) was introduced into the sample in a stepwise manner. The red solution of [(TrPP)$Fe^{II}(py)_2$] turned brownish on addition of the hydrogen peroxide, and the ^1H NMR spectra showed the gradual growth of a new set of resonances accompanied by a lowering of the intensities of those assigned to the low-spin diamagnetic [(TrPP)Fe^{II}-$(py)_2$]. A paramagnetic product was identified as (5-oxo-10,15,20-triphenylphlorin)iron with two axially coordinated [D_5]pyridine ligands, [(5-O-TrPP)Fe$(py)_2$] (see below). Thus, the reaction had taken place exclusively at the unsubstituted *meso* position. Once formed, the solution of [(5-O-TrPP)Fe$(py)_2$] in [D_5]pyridine is stable as long as it is protected from dioxygen, the addition of which results in bleaching.

Extraction of the [D_5]pyridine solution of [(5-O-TrPP)Fe$(py)_2$] with 1 M aqueous HCl yielded high-spin [(5-OH-TrPP)Fe^{III}Cl]. Subsequently, the dichloromethane solution of [(5-OH-TrPP)Fe^{III}Cl] was subjected to chromatography on a silica column. In the course of the process the monomeric [(5-OH-TrPP)Fe^{III}Cl] complex was transformed into the cyclic dimer [(5-O-TrPP)$Fe^{III}]_2$ (Scheme 3).

Coupled Oxidation

Recently, a convenient method for the preparation of the dimeric [(OEPO)$Fe^{III}]_2$ complex has been reported in the course of coupled oxidation of [(OEP)Fe^{III}Cl] under pyridine-free conditions.[48] Herein, this procedure has been adopted with success to obtain [(5-O-TrPP)$Fe^{III}]_2$.

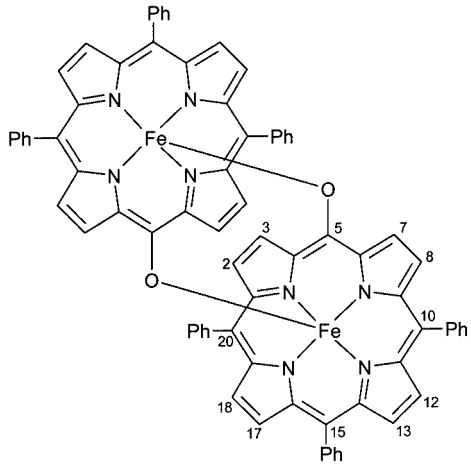

Scheme 3

Addition of [(TrPP)Fe^{III}Cl] to a methanolic solution of ascorbic acid and potassium cyanide leads to oxidative hydroxylation of the porphyrin ring to form [(5-O-TrPP)Fe^{III}]$_2$. Initially, the cyanide coordinates to [(TrPP)Fe^{III}Cl] producing [(TrPP)$Fe^{III}(CN)_2]^-$, a reaction substrate that is soluble in methanol. The reaction mixture was stirred overnight in the presence of air. In the course of the coupled oxidation we obtained [(5-O-TrPP)Fe^{III}]$_2$, which was subsequently separated using column chromatography. The yield of the process was ca. 20%. At the present stage of investigations, no effort has been made to optimize the yield and to characterize other feasible reaction products.

Characterization of [(5-O-TrPP)Fe^{III}]$_2$

The electronic spectrum of [(5-O-TrPP)Fe^{III}]$_2$ is presented in Figure 3 together with the spectrum of [(5-OAc-TrPP)Fe^{III}Cl] and [(5-O-TrPP)Fe$(CN)_2]^{2-}$ (see below). The electronic spectrum of [(5-OAc-TrPP)Fe^{III}Cl] resembles the spectra of high-spin (tetraphenylporphyrin)iron(III) complexes and other [(5-X-TrPP)Fe^{III}Cl] complexes. The electronic spectrum of [(5-O-TrPP)Fe^{III}]$_2$ is considerably different; all bands are broadened compared to [(5-OAc-TrPP)Fe^{III}Cl], and a new band is detected at 330 nm. These differences may be induced by the 5-oxygen axial ligand coordination[49] and/or from the porphyrin−porphyrin π interaction caused by the proximity of the porphyrin rings in the close-packed dimeric structure.[13,16,50−52]

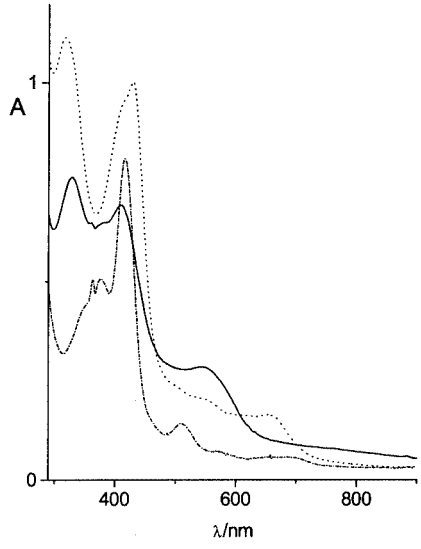

Figure 3. Electronic absorption spectra of [(5-O-TrPP)Fe^{III}]$_2$ (——), [(5-AcO-TrPP)Fe^{III}Cl] (-·-·-·) (both in CH_2Cl_2), and [(5-O-TrPP)Fe$(CN)_2]^{2-}$ (· · ·) (in methanol)

The electrospray ionization (ESI) mass spectrum of [(5-O-TrPP)Fe^{III}]$_2$ shows peaks due to the parent species [(5-O-TrPP)Fe^{III}]$_2$ at *m*/*z* (%) = 1215.4 (7) and its deoligmerization product [(5-OH-TrPP)$Fe^{III}]^+$ at *m*/*z* (%) = 608.3 (100). In our experiment the most intense peak corresponds to the monomeric unit because the technique used requires the addition of acid to the sample, which favors the formation of monomer.

^{1}H NMR Spectroscopic Studies of [(5-O-TrPP)Fe^{III}]$_2$

The downfield part of the ^{1}H NMR spectrum of [(5-O-TrPP)Fe^{III}]$_2$ is shown in Figure 4 (Trace A). The resonance assignments have been made on the basis of relative intensities and linewidth analysis. The ^{1}H NMR spectrum of [(5-O-TrPP)Fe^{III}]$_2$ shows a number of remarkable features that must arise from its unusual molecular structure. In particular, three β-pyrrolic signals are strongly displaced upfield relative to their typical position for the high-spin (tetraphenylporphyrin)iron(III) complexes at δ (linewidths in Hz) = 56.3 (400), 49.6 (650), 47.5 (2200) ppm ($CDCl_3$, 293 K). The deconvolution procedure (not shown) has been applied to this part of the spectrum in order to demonstrate that three resonances of remarkably different linewidths and identical intensities are required to reproduce the experimental spectrum. The fourth inequivalent pyrrole position produces the resonance at δ = 84.3 (linewidth 300 Hz) ppm. The phenyl resonances form a complex, unresolved pattern which is spread over the δ = 0−16 ppm range.

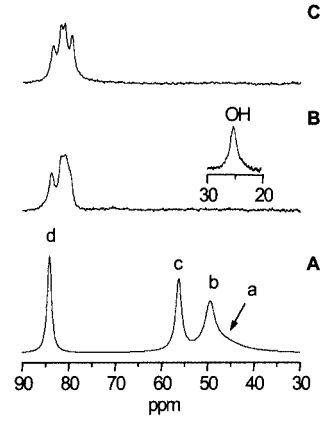

Figure 4. The downfield region of (A) 300 MHz ^{1}H NMR spectrum of [(5-O-TrPP)Fe^{III}]$_2$ at 291 K, (B) 500 MHz ^{1}H NMR spectrum of [(5-OH-TrPP)Fe^{III}Cl], (C) 500 MHz ^{1}H NMR spectrum of [(5-AcO-TrPP)Fe^{III}Cl]; resonance assignments: a: 3(7)-H; b: 2(8)-H; c: 12(18)-H; d: 13(17)-H

Molecular mechanics calculations have been used to visualize the structure of the dimer and to estimate the degree of the porphyrin distortion that is necessary to form this species. In the minimization procedure we used the standard MM+ parameterization of the HyperChem program, with the exception of the iron coordination surroundings where we imposed the constraints reflecting the high-spin state of the iron(III) ion. The characteristic features of the high-spin (tetraphenylporphyrin)iron(III) complexes and [(5-Br-TrPP)Fe^{III}Cl] included displacement of the iron ion from the plane of the four nitrogen atoms (0.45 Å), and relatively long Fe−N bonds (2.05 Å).[41−43] The spectroscopic evidence indicates that the iron(III) complex has a head-to-tail dimeric structure, with the *meso*-alkoxide groups forming the bridges from one macrocycle to the metal ion of the adjacent macrocycle. Such a dimeric structure accounts for the mass of the largest ion in the mass spectrum. The ^{1}H NMR spectrum clearly shows the equivalence of the two (porphyrin)iron(III) subunits. The upfield relocation of three β-H resonances can be explained only by the direct coordination of the O(5) atom to the external iron(III) ion, as required by the cyclic dimeric structure. Hence high-spin (5-hydroxytriphenylporphyrin)-iron(III) can be used as a building block in the dimerization.

A schematic view of the dimeric (porphyrin)iron(III) skeleton as obtained by molecular mechanics is presented in Figure 5. The closest contacts are in the range observed in the structures of other metalloporphyrins.[15,19,41]

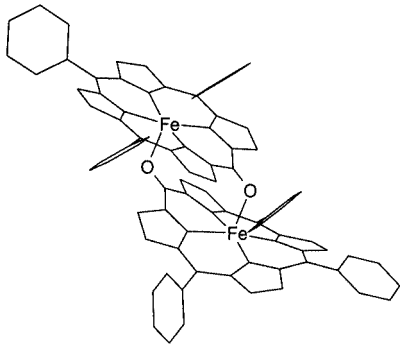

Figure 5. Drawing of the dimer [(5-O-TrPP)Fe^{III}]$_2$ obtained from the molecular mechanics calculations; hydrogen atoms have been omitted for the sake of clarity

The features of the ^{1}H NMR spectra of [(5-O-TrPP)Fe^{III}]$_2$ can be understood in the context of the presence of two high-spin iron(III) ions in the molecule. The 5-hydroxyporphyrin of each monomeric unit is coordinated simultaneously to the internal iron(III) ion through the four nitrogen atoms and to the external one by the 5-oxygen atom. The typical delocalization pathway for high-spin (tetraphenylporphyrin)iron(III) complexes shifts the pyrrole resonances downfield as a result of the dominating σ-contact contribution. Additionally, the π delocalization locates a considerable amount of the spin density at the *meso* positions,[16,31,53−55] and some at the pyrrole positions.[56] The π-spin density at the *meso*-carbon atoms produces sign alternation of the *meso*-phenyl resonances. The dipolar contribution, caused only by the ZFS effect in high-spin (porphyrin)iron complexes, is usually notably smaller than the contact contribution, and this observation has been applied in the further analysis of the hyperfine shifts.[55]

The characteristic features of the internal iron(III) ion influence are exemplified by the ^{1}H NMR spectra of [(5-X-TrPP)Fe^{III}I] (X = NO_2, Br, MeO, H; the choice of I^- as an axial ligand allowed better differentiation of the pyrrole resonances), [(5-OH-TrPP)Fe^{III}Cl], and [(5-AcO-TrPP)-Fe^{III}Cl], where the typical downfield sets of the four pyrrole resonances are found centered around δ = 80 ppm (as shown in traces B and C of Figure 4, and in Table 1). The presence of a second source of spin density in [(5-O-TrPP)Fe^{III}]$_2$, i.e., the external iron(III) ion, changes the hyperfine shifts for the β-H pyrrole protons considerably. Assuming simple additivity of contact contributions by two independent routes, we have estimated that such shifts require a downfield contribution similar to that found for [(5-OH-TrPP)Fe^{III}Cl], hence the upfield shift of ca. −30 ppm for 2(8)-H, −32 ppm for 3(7)-H, and −24 ppm for 12(18)-H. This upfield contribution to the β-H shift results mainly from the σ donation of the electron density of the 5-oxygen donor on the half-occupied d_{z^2} orbital of the iron(III) ion. The anticipated positive spin density on the σ orbital of the oxygen atom will be directly transferred into the π system of the pyrrole ring without any iron(III)−oxygen π bonding, spreading the effect up to the distant pyrrole position [12(18)-H] with respect to the coordinating oxygen atom. The σ orbital of the oxygen atom and the porphyrin π orbitals are not orthogonal, and consequently σ−π overlap permits the direct spin-density transfer.[57,58] We therefore suggest a similar delocalization mechanism to that proposed for [(2-O-TPP)Fe^{III}]$_3$, although with a different location of the external coordinating center.[16]

The linewidths of the β-H pyrrole resonances correlate with their specific locations within the dimeric structure. The dipolar contribution to linewidth broadening is presumed to be proportional to r^{-6}, where r is the distance from the paramagnetic iron(III) center to the proton in question when the ligand-centered dipolar relaxation is insignificant.[59,60] The contribution from the internal iron(III) ion by dipolar and scalar mechanisms has been approximated by the linewidths of the most downfield pyrrole resonance. The markedly larger linewidths of the β-H resonances can be split into two parts: the internal one, which is identical to the most downfield pyrrole position, and the remaining external one {100 Hz [12(18)-H], 350 Hz [2(8)-H], and 1900 Hz [3(7)-H]}. Most likely the external part derives mainly from the dominant dipolar relaxation of the neighboring external iron(III) ion. The respective $Fe_{external}$−β-H distances are estimated from the model to be: 3.5 Å (3/7-H), 5.5 Å (2/8-H), 9 Å (12/18-H), 10 Å (13/17-H). Thus, the pattern of pyrrole linewidths is qualitatively in agreement with the proposed molecular structure.

Table 1. ^{1}H NMR chemical shifts of the pyrrole resonances of *meso*-substituted high-spin (triphenylporphyrin)iron(III) complexes

Compound	δ [ppm][a]
[(5-NO_2-TrPP)Fe^{III}I]	80.0 (2 H), 80.2 (2 H), 84.5 (4 H)
[(5-Br-TrPP)Fe^{III}I]	81.1 (2 H), 82.2 (4 H), 85.3 (2 H)
[(5-MeO-TrPP)Fe^{III}I]	88.2 (2 H), 92.8 (2 H), 93.7 (2 H), 94.5 (2 H)
[(5-OH-TrPP)Fe^{III}Cl]	79.9 (2 H), 80.8 (2 H), 81.7 (2 H), 83.8 (2 H)
[(5-AcO-TrPP)Fe^{III}Cl]	79.4 (2 H), 80.9 (2 H), 81.9 (2 H), 83.5 (2 H)
[(5-O-TrPP)Fe^{III}]$_2$	47.5 (4 H), 49.6 (4 H), 56.3 (4 H), 84.3 (4 H)

[a] Conditions: T = 293 K, $CDCl_3$, 500 MHz or 300 MHz.

Cleavage of [(5-O-TrPP)Fe^{III}]$_2$

Addition of acids in excess to [(5-O-TrPP)Fe^{III}]$_2$ results in the cleavage of the dimer according to Equation (1).

$$[(5\text{-O-TrPP})Fe^{III}]_2 + 2\,HX \rightarrow 2\,[(5\text{-OH-TrPP})Fe^{III}X] \quad (X = Cl, TFA) \qquad (1)$$

Trace B of Figure 4 shows the spectrum of a [(5-O-TrPP)Fe^{III}]$_2$ sample to which gaseous HCl has been added. The spectrum is consistent with the formation of [(5-OH-TrPP)Fe^{III}Cl]. The β-H pyrrole resonances of [(5-O-TrPP)Fe^{III}]$_2$ centered at δ = 50 ppm disappeared. Four new pyrrole resonances were found (δ = 83.8, 81.7, 89.0, 79.9 ppm). They correspond to four pyrrole protons that are inequivalent because of the 5-substitution. The pyrrole resonances of [(5-OH-TrPP)Fe^{III}Cl] have similar linewidths (ca. 600 Hz). The differential broadening of the pyrrole resonances determined for the dimeric molecule is absent. A unique resonance at δ = 25.3 ppm for [(5-OH-TrPP)Fe^{III}Cl] has been assigned to the 5-hydroxy proton {the intensity of this resonance varies in the range 1−2 H depending on preparation, so the formation of [(5-H_2O-TrPP)FeCl]$^+$ remaining in the fast equilibrium with [(5-OH-TrPP)Fe^{III}Cl] seems to be of importance}. When a small amount of $CDCl_3$, saturated with deuterium oxide, was added to the solution of [(5-OH-TrPP)Fe^{III}Cl], the 5-OH resonance diminished in intensity. Addition of base to [(5-OH-TrPP)Fe^{III}Cl] caused its conversion into [(5-O-TrPP)Fe^{III}]$_2$. Actually, such a conversion was detected even when a $CDCl_3$ solution of [(5-OH-TrPP)Fe^{III}Cl] was saturated with water.

[(5-O-TrPP)Fe^{III}]$_2$ was also split with acetic anhydride into (5-acetoxy-10,15,20-triphenylporphyrin)iron(III). The relevant ^{1}H NMR spectrum of the resulting complex, [(5-AcO-TrPP)Fe^{III}Cl] is presented in trace C of Figure 4. The feasible formation of two isomeric forms, one with the carbonyl oxygen atom and the chloride ion on the same side of the porphyrin, and one with these groups on the opposite faces of the porphyrin plane cannot be excluded, although they have not been confirmed by ^{1}H NMR spectroscopy because the respective β-H resonances are not sufficiently resolved.

Cleavage of [(5-O-TrPP)Fe^{III}]$_2$ by Pyridine or Cyanide Anion

In the presence of [D_5]pyridine, [(5-O-TrPP)Fe^{III}]$_2$ undergoes a cleavage to form air-sensitive [(5-O-TrPP)Fe(py)$_2$]. Thus, treatment of a dioxygen-free chloroform solution of the dimeric complex with a 50-fold excess of [D_5]pyridine results in its immediate conversion. The overall pattern of resonances is similar to that generated in the hydroxylation of [(TrPP)Fe^{II}(py)$_2$]. The detected shift differences have been attributed to the solvent effect and/or a different concentration of the pyridine ligand remaining in equilibrium. The ^{1}H NMR spectrum of the [D_5]pyridine solution of [(5-O-TrPP)Fe(py)$_2$] is shown in Figure 6, and the chemical shifts are given in Table 2. Three of the four pyrrole resonances are found in the downfield region of the spectrum, while the other signal is located upfield. Sign alternation of isotropic shifts of *meso*-phenyl protons is also observed, with larger absolute shift values assigned to the 15-Ph position.

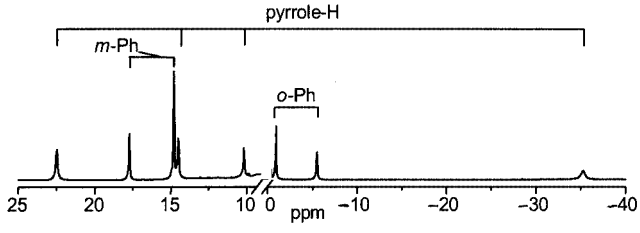

Figure 6. 500 MHz ^{1}H NMR spectrum of [(5-O-TrPP)Fe(py)$_2$] in a [D_5]pyridine solution; resonance assignment: pyrrole-H: pyrrole protons; *o*-Ph, *m*-Ph: *ortho*-, *meta*-phenyl protons

A ^{1}H NMR titration was carried out by addition of trifluoroacetic acid (solution in $CDCl_3$) to a solution of [(5-O-TrPP)Fe(py)$_2$] in [D_5]pyridine. Smooth changes of the chemical shifts in the whole titration range were observed. This fact can be attributed to a gradual protonation of the 5-oxygen atom and a fast proton exchange among two species in the system formed in the conditions of our experiment, as shown in Equation (2).

$$(5\text{-O-TrPP})Fe(py)_2 + H^+ \rightleftarrows [(5\text{-OH-TrPP})Fe^{III}(py)_2]^+ \qquad (2)$$

The direction of shift changes experienced by the pyrrole resonances indicates that protonation of the 5-O atom results in the formation of a low-spin complex [(5-OH-TrPP)Fe^{III}(py)$_2$]$^+$ with the usual $(d_{xy})^2(d_{xz},d_{yz})^3$ electronic ground state. Independently, this complex was observed in the course of [D_5]pyridine titration of [(5-OH-TrPP)Fe^{III}-(TFA)] conducted in $CDCl_3$, and is characterized by four

Table 2. ^{1}H NMR chemical shifts of bis(pyridine) and bis(cyanide) complexes[a]

Compound	δ [ppm] pyrrole-H 2(8)-H	3(7)-H	12(18)-H	13(17)-H	*ortho*-Ph 10(20)-H	15-H	*meta*-Ph 10(20)-H	15-H	*para*-Ph 10(20)-H	15-H	Solvent
[(5-O-TrPP)Fe(py)$_2$]	−35.4	22.6	10.2, 14.6[b]		−0.8	−5.5	14.9	17.8	2.2	−0.3	C_5D_5N
[(5-O-TrPP)Fe(py)$_2$]	−30.2	21.0	13.6, 14.6[b]		−0.7	−4.6	14.6	17.2	[b]	0.1	$CDCl_3$
[(5-O-TrPP)Fe(CN)$_2$]$^{2-}$	−6.0	12.9	8.1, 9.1[b]		2.2	0.2	12.9	13.7	4.1	3.0	CD_3OD
[(5-NO_2-TrPP)Fe^{III}(CN)$_2$]$^-$	−13.9	−9.6	−14.4	−15.1	6.0	4.6	7.3	6.7	6.7	6.3	CD_3OD
[(5-Br-TrPP)Fe^{III}(CN)$_2$]$^-$	−7.5	−6.9	−8.5	−7.9	5.6	5.4	8.2	8.0	6.5	6.4	CD_3OD
[(5-MeO-TrPP)Fe^{III}(CN)$_2$]$^-$ [c]	−6.6	−5.9	−7.0	−7.4	5.5	5.3	8.8	8.6	6.3	6.3	CD_3OD

[a] Conditions: T = 293 K, 500 MHz. Intensities: pyrrole resonances (2 H each); 10(20)-*ortho* and 10(20)-*meta*-Ph (4 H); 15-*ortho*, 15-*meta*, and 10-*para*-Ph (2 H); 15-*para*-Ph (1 H). [b] Not identified. [c] MeO resonance at δ = 2.9 ppm.

upfield pyrrole resonances [δ = −16.8, −19.8, −27.4, −27.8 ppm (293 K)].

In the presence of a large excess of the cyanide ion [(5-O-TrPP)Fe^{III}]$_2$, dissolved in [D_4]methanol, undergoes cleavage to form the air-sensitive [(5-O-TrPP)Fe(CN)$_2$]$^{2-}$. The ^{1}H NMR spectrum of the resulting solution is shown in Figure 7. The overall pattern of resonances with three downfield and one upfield pyrrole resonances [δ = 12.9, 9.1, 8.1, −6.0 ppm (293 K)] is similar to that of [(5-O-TrPP)Fe(py)$_2$]. The sign alternation of the isotropic shifts of the *meso*-phenyl resonances has also been detected. Since only two *ortho* resonances are observed, the axial ligation on both sides of the macrocycle is identical.

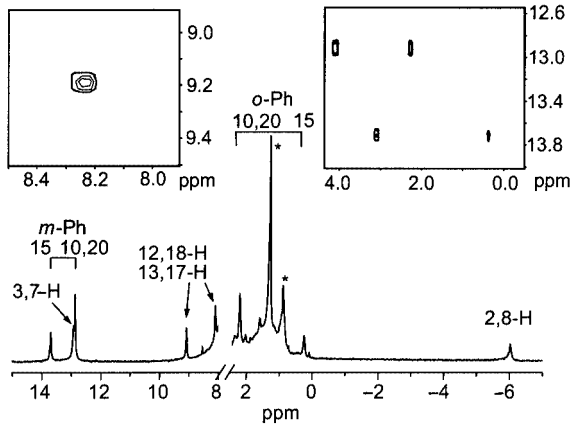

Figure 7. 500 MHz ^{1}H NMR spectrum of [(5-O-TrPP)Fe(CN)$_2$]$^{2-}$ in [D_4]methanol (293 K); the insets show the respective COSY maps; resonance assignments as in Figure 6

The insets in Figure 7 show fragments of a COSY spectrum that was obtained for [(5-O-TrPP)Fe(CN)$_2$]$^{2-}$. The individual *meso*-phenyl groups were identified by the respective cross-peaks between the *ortho*, *meta*, and *para* protons. The cross-peak detected between the pyrrole resonances at δ = 8.1 and 9.1 ppm confirms their location on the same pyrrole ring. Consequently, two other pyrrole resonances are assigned to a second scalar-coupled pair of pyrrole resonances.

The UV/Vis absorption spectrum of [(5-O-TrPP)Fe(CN)$_2$]$^{2-}$ is included in Figure 3. The spectrum displays the Soret band at 427 nm and a broad absorption at 659 nm.

Electronic Structure of [(5-O-TrPP)Fe(py)$_2$] and [(5-O-TrPP)Fe(CN)$_2$]$^{2-}$

Addition of an excess of potassium cyanide to a solution of [(5-X-TrPP)Fe^{III}Cl] in [D_4]methanol results in its conversion into the six-coordinate low-spin complex [(5-X-TPP)Fe^{III}(CN)$_2$]$^-$. The representative ^{1}H NMR spectra for [(5-X-TPP)Fe^{III}(CN)$_2$]$^-$ complexes (the pyrrole region) are shown in Figure 8, and the chemical shift values are gathered in Table 2. The characteristic sets of four upfield-shifted pyrrole resonances assigned by means of 2D NMR experiments have been observed for each compound. These resonances are accompanied by sets of upfield-shifted *ortho* and *para* proton resonances of the *meso*-phenyl groups and downfield shifted *meta* proton signals. The ^{1}H NMR spectra reflect features typical for low-spin (porphyrin)iron(III) complexes.[31,56]

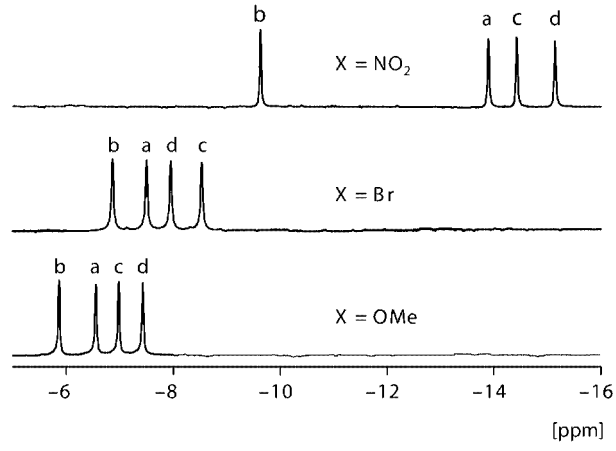

Figure 8. 500 MHz ^{1}H NMR spectra (pyrrole region) of [(5-X-TrPP)Fe^{III}(CN)$_2$]$^-$ complexes (X = NO_2, Br, MeO) in a [D_4]methanol solution at 293 K; resonance assignments follow those of Figure 4

On the contrary, the ^{1}H NMR spectrum of [(5-O-TrPP)Fe(CN)$_2$]$^{2-}$ demonstrates the remarkably different pattern revealing the sign alternation detected for the pyrrole resonances (Figure 7). The overall oxidation level of

[(5-O-TrPP)Fe(py)$_2$] or [(5-O-TrPP)Fe(CN)$_2$]$^{2-}$ is consistent with the resonance structures presented in Scheme 4.[12,21−27,48]

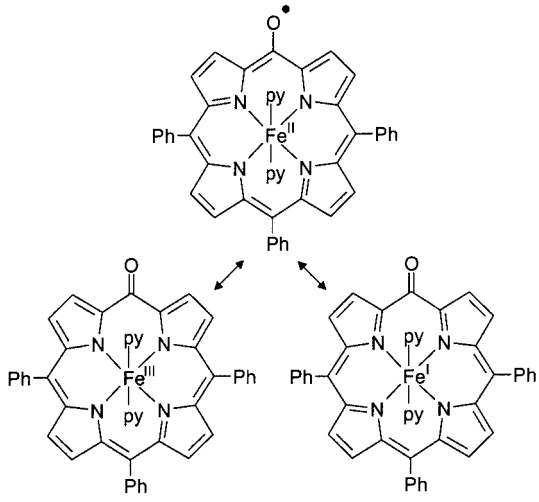

Scheme 4

The new (oxophlorin)iron complexes [(5-O-TrPP)Fe(py)$_2$] and [(5-O-TrPP)Fe(CN)$_2$]$^{2-}$ present ^{1}H NMR spectroscopic patterns that reveal a general similarity to the spectra of [(OEPO)Fe(py)$_2$], [(5-X-OEPO)Fe(py)$_2$], [(OEPO)Fe(CN)$_2$]$^{2-}$, [(Etio-I-PO)Fe(py)$_2$], [(DeuteroPO)Fe(py)$_2$], [(MesoPO)Fe(py)$_2$], and [(ProtoPO)Fe(py)$_2$] (OEPO, 5-X-OEPO, Etio-I-PO, DeuteroPO, MesoPO, and ProtoPO are trianions of oxophlorins obtained from octaethylporphyrin, 5-substituted octaethylporphyrin, etioporphyrin-I, deuteroporphyrin-IX dimethyl ester, mesoporphyrin-IX dimethyl ester, and protoporphyrin-IX dimethyl ester, respectively).[22,26,46]

Based on the chemical shifts measured for the four (deuterooxophlorin)iron isomers [(DeuteroPO)Fe(py)$_2$], the following values are anticipated for (5-oxophlorin)iron or its β-methylated derivative: pyrrole resonances: δ = −33 (2-H), 27 (3-H), 13 (12- and 13-H) ppm; methyl resonances: δ = 65 (2-CH$_3$), −14 (3-CH$_3$) ppm. Substitution of a methyl group by a proton is expected to give rise to a resonance that is subject to a hyperfine shift of opposite sign, but a magnitude similar to that of the corresponding methyl group if π-spin delocalization dominates the hyperfine shifts. Consequently, the pyrrole β-H resonances with the largest hyperfine shifts and the methyl resonances with the most upfield shift must originate from a common site (i.e., from a site with similar value and sign of the spin density) within the molecule as has been well documented for four regioisomers of [(DeuteroPO)Fe(py)$_2$].[26]

The four pyrrole protons of [(5-O-TrPP)Fe(py)$_2$] provide direct probes of the spin density around the oxophlorin macrocycle. In principle, this should allow the determination of the differences in the contact shifts for four pyrrole rings avoiding any differences due to the unsymmetrical substitution effect expected for natural porphyrins. The pyrrole pattern determined for [(5-O-TrPP)Fe(py)$_2$] was found to be very similar to that determined from the rather complex analysis carried out for four (oxophlorin)iron regioisomers obtained from hemes.[26] The relatively large paramagnetic shift of the *meso*-phenyl resonances dominated by the π-contact mechanism reflects the large spin density at the *meso* positions, as found previously for other (oxophlorin)-iron complexes. In conclusion, the spin-density distribution

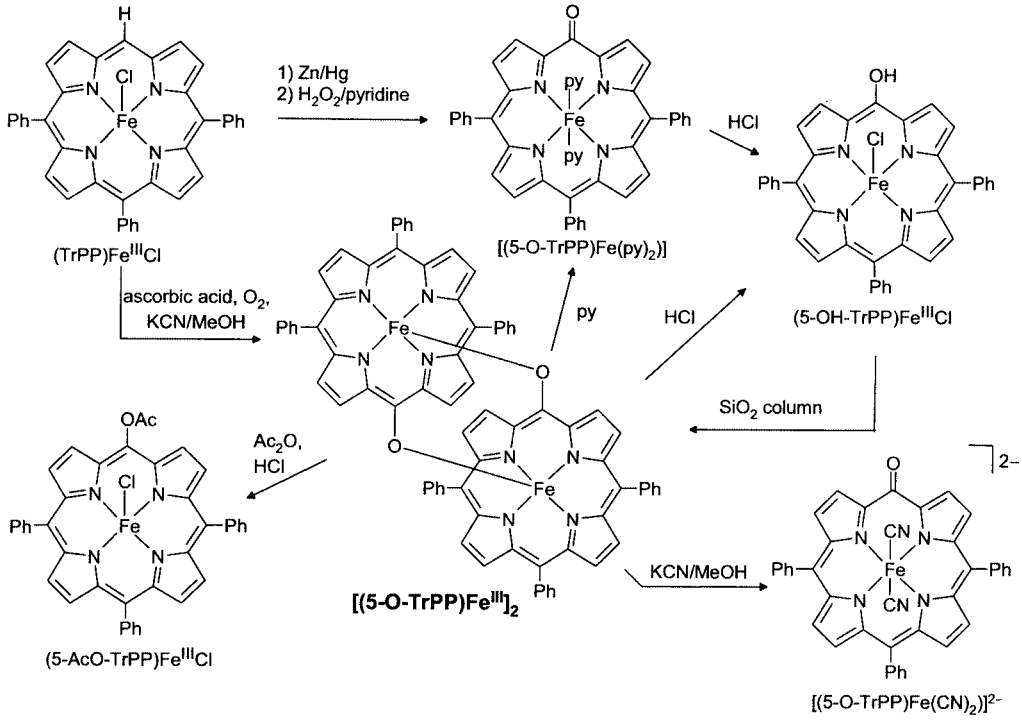

Scheme 5

in the oxophlorin skeleton is dominated by the location of the oxygenated *meso* site and that this functional group imposes a basic twofold electronic symmetry that is only moderately perturbed by the presence of other functional groups.

Conclusion

The synthetic work of this contribution is summarized in Scheme 5. In particular, this work demonstrates considerable parallels in the properties of (10,15,20-triphenyl-5-oxophlorin)iron and (oxophlorin)iron complexes completely substituted at the β-positions. Potentially, an introduction of the *meso*-phenyl groups provides a suitable means for the control and exploration of the properties of this peculiar class of (porphyrin)iron-related systems. The electronic and steric factors can be conveniently adjusted by appropriate substitution of the *meso*-phenyl rings.

Experimental Section

General: ^{1}H NMR spectra were recorded with a Bruker AMX300 and a Bruker Avance 500 spectrometer operating at 300 and 500 MHz, respectively. The residual ^{1}H resonances of the deuterated solvents were used as internal references. Absorption spectra were recorded with a diode-array Hewlett Packard 8453 spectrometer. Mass spectra were recorded with a Finnigan MAT TSQ 700 spectrometer using the ESI technique. Molecular mechanics calculations using the HyperChem software (Autodesk) were carried out and displayed with a Pentium PC. The standard MM+ force field, with the constraints set on the coordination bonds to achieve a high-spin (porphyrin)iron(III) geometry, were used as described in the text. 5,10,15-Triphenylpophyrin ($TrPPH_2$) and 5-bromo-10,15,20-triphenylporphyrin (5-Br$TrPPH_2$) were synthesized as described previously.[35,36,38,45] 5-Nitro-10,15,20-triphenylporphyrin (5-NO_2-$TrPPH_2$) was obtained by nitration of $TrPPH_2$ with $AgNO_2$ in the presence of I_2 by modification of the method applied for nitration of 5,15-diphenylporphyrin.[39]

5-Methoxy-10,15,20-triphenylporphyrin: [(TrPP)Zn^{II}] (40 mg) was dissolved in 50 mL of toluene, and sodium methoxide (1−2 g) was added along with a small amount of methanol. The mixture was refluxed in the presence of air for 6 h and then concentrated to dryness under reduced pressure. The solid residue was extracted with a small volume of CH_2Cl_2, and the dissolved crude product was column-chromatographed on basic alumina with dichloromethane. [(5-MeO-TrPP)Zn^{II}] was eluted as the second band, directly after the unchanged [(TrPP)Zn^{II}]. The zinc complex of 5-methoxy-10,15,20-triphenylporphyrin was demetallated with hydrochloric acid to yield 5-MeO-$TrPPH_2$, which was used without further purification. ^{1}H NMR ($CDCl_3$): δ = −2.70 (s, 2 H, NH), 4.95 (s, 3 H, OCH_3), 7.7 (m, 9 H, *m*,*p*-Ph), 8.2 (m, 6 H, *o*-Ph), 8.76 (d, ^3J = 4.8 Hz, 2 H, H_β), 8.81 (d, ^3J = 4.8 Hz, 2 H, H_β), 8.88 (d, ^3J = 4.8 Hz, 2 H, H_β), 9.53 (d, ^3J = 4.8 Hz, 2 H, H_β) ppm. MS (ESI): *m*/*z* (%) = 569.5 (100) [MH^+].

Iron ion insertion according to a known route yielded the corresponding [(5-X-TrPP)Fe^{III}Cl] complexes.[16,56] Usually, the dicyano-ligated complexes of the investigated (porphyrin)iron(III) complexes were prepared by dissolution of 2−3 mg of the respective high-spin complex in 0.4 mL of [D_4]methanol saturated with KCN.

[Fe^{III}(OEPO)]$_2$: Potassium cyanide (43.7 mg, 0.67 mmol) and ascorbic acid (0.53 g, 3.0 mmol) were dissolved in 50 mL of methanol. [(TrPP)Fe^{III}Cl] (41 mg, 0.065 mmol) was added to the solution, and the reaction mixture was stirred in air for 12−20 h. The resulting solution was concentrated to a volume of 5 mL, diluted with 10 mL of dichloromethane, and washed 2−3 times with water. The organic layer was dried and the solvents were evaporated to dryness. The crude sample was column-chromatographed on silica gel (0.05−0.2 mm/70−270 mesh). The dimeric complex was eluted with an ethanol/dichloromethane mixture (2:98, v/v), and recrystallized from dichloromethane/hexane. Yield: 8 mg (20%). MS (ESI): *m*/*z* (%) = 1215.4 (7) [M^+], 608.3 (100) [(5-OH-TrPP)Fe^{III}]$^+$.

X-ray Crystallographic Study: Crystals of $TrPPH_2$ were grown by slow diffusion of *n*-hexane into a dichloromethane solution of the porphyrin. Diffraction data were collected with a Kuma KM4CCD diffractometer. The data were corrected for Lorentz and polarization effects. No absorption correction was applied. The structure was solved by direct methods (SHELXS-97) and refined by full-matrix least squares (SHELXL-97). All heavy atoms were refined anisotropically and the hydrogen atoms isotropically with no constraints. Crystals of [(5-Br-TrPP)Fe^{III}Cl]·C_6H_6 were obtained by slow concentration of a CH_2Cl_2/benzene solution. The specimen chosen for analysis was twinned but the diffraction patterns of the two domains did not overlap significantly. Data collection was carried out as for $TrPPH_2$. The structure was solved using heavy-atom methods (SHELXS-97) and refined by full-matrix least squares (SHELXL-97). Heavy atoms were refined anisotropically, and the hydrogen atoms by using a riding model. Empirical absorption correction assuming an ellipsoidal crystal was applied using the routine implemented in XPREP.[61] Crystal data and details of the data collection and refinement are presented in Table 3. CCDC-173923 and -173924 contain the supplementary crystallographic data for

Table 3. Crystal data for $TrPPH_2$ and [(5-Br-TrPP)Fe^{III}Cl]·C_6H_6

	$TrPPH_2$	[(5-Br-TrPP)Fe^{III}Cl]·C_6H_6
Empirical formula	$C_{38}H_{26}N_4$	$C_{41}H_{26}N_4BrClFe$
Formula mass	538.63	745.87
a [Å]	6.5811(11)	11.341(2)
b [Å]	18.344(3)	12.994(3)
c [Å]	22.622(4)	13.626(3)
α [°]	90	107.96(3)
β [°]	90	103.66(3)
γ [°]	90	111.34(3)
V [Å^3]	2731.1(8)	1635.9(6)
Z	4	2
$D_{calcd.}$ [g·cm^{-3}]	1.310	1.514
Crystal system	orthorhombic	triclinic
Space group	$P2_12_12_1$	$P\bar{1}$
Crystal size [mm]	0.5 × 0.3 × 0.2	0.2 ×0.15 × 0.1
μ [mm^{-1}]	0.078	1.801
T_{min}, T_{max}	0.962, 0.985	0.728, 0.921
T [K]	100(2)	100(2)
θ range [°]	2.86 ≤ θ ≤ 29.07	2.66 ≤ θ ≤ 28.98
hkl range	−8 ≤ *h* ≤ 5	−11 ≤ *h* ≤ 15
	−24 ≤ *k* ≤ 24	−17 ≤ *k* ≤ 16
	−30 ≤ *l* ≤ 30	−18 ≤ *l* ≤ 18
Reflections measured	18512	12048
unique [$I \geq 2\sigma(I)$]	5117	5734
Parameters/restraints	484/1	433/0
*R*1	0.0685	0.0665
*wR*2	0.1411	0.1512
S	1.068	1.096

this paper. These data can be obtained free of charge at www.ccdc.cam.ac.uk/conts/retrieving.html or from the Cambridge Crystallographic Data Centre, 12, Union Road, Cambridge CB2 1EZ, UK [Fax: (internat.) + 44-1223/336-033; E-mail: deposit@ccdc.cam.ac.uk].

Acknowledgments

Financial support from the State Committee for Scientific Research KBN of Poland (Grant 3 T09A 155 15) and the Foundation for Polish Science is kindly acknowledged.

[1] J. Wojaczyński, L. Latos-Grażyński, *Coord. Chem. Rev.* **2000**, *204*, 113.
[2] T. Imamura, K. Fukushima, *Coord. Chem. Rev.* **2000**, *198*, 133.
[3] A. K. Burrell, D. L. Officer, P. G. Plieger, D. C. W. Reid, *Chem. Rev.* **2001**, *101*, 2751.
[4] G. H. Barnett, M. F. Hudson, S. W. McCombie, K. M. Smith, *J. Chem. Soc., Perkin Trans. 1* **1973**, 691.
[5] R. G. Little, J. A. Anton, P. A. Loach, J. A. Ibers, *J. Heterocycl. Chem.* **1975**, *12*, 343.
[6] H. Callot, *Bull. Soc. Chim. Fr.* **1974**, 1492.
[7] M. J. Crossley, L. G. King, S. M. Pyke, *Tetrahedron* **1987**, *43*, 4569.
[8] H. M. Goff, E. T. Shimomura, Y. J. Lee, W. R. Scheidt, *Inorg. Chem.* **1984**, *23*, 315.
[9] G. M. Godziela, D. Tilotta, H. M. Goff, *Inorg. Chem.* **1986**, *25*, 2142.
[10] N. Masuoka, H. A. Itano, *Biochemistry* **1987**, *26*, 3672.
[11] S. I. Beale, *Chem. Rev.* **1993**, *93*, 785.
[12] A. L. Balch, *Coord. Chem. Rev.* **2000**, *200−202*, 349.
[13] A. L. Balch, L. Latos-Grażyński, B. C. Noll, M. M. Olmstead, E. P. Zovinka, *Inorg. Chem.* **1992**, *31*, 2248.
[14] A. L. Balch, B. C. Noll, S. M. Reid, E. P. Zovinka, *Inorg. Chem.* **1993**, *32*, 2610.
[15] A. L. Balch, B. C. Noll, M. M. Olmstead, S. M. Reid, *J. Chem. Soc., Chem. Commun.* **1993**, 1088.
[16] J. Wojaczyński, L. Latos-Grażyński, *Inorg. Chem.* **1995**, *34*, 1044.
[17] J. Wojaczyński, L. Latos-Grażyński, *Inorg. Chem.* **1995**, *34*, 1054.
[18] J. Wojaczyński, L. Latos-Grażyński, *Inorg. Chem.* **1996**, *35*, 4812.
[19] J. Wojaczyński, L. Latos-Grażyński, M. M. Olmstead, A. L. Balch, *Inorg. Chem.* **1997**, *36*, 4548.
[20] P. S. Clezy, in: *The Porphyrins* (Ed.: D. Dolphin), Academic Press, New York, **1978**, vol. 2, p. 103.
[21] S. Sano, Y. Sugiura, Y. Maeda, S. Ogawa, I. Morishima, *J. Am. Chem. Soc.* **1981**, *103*, 2888.
[22] S. Sano, T. Sano, I. Morishima, Y. Shiro, Y. Maeda, *Proc. Natl. Acad. Sci. U. S. A.* **1986**, *83*, 531.
[23] I. Morishima, H. Fujii, Y. Shiro, S. Sano, *J. Am. Chem. Soc.* **1986**, *108*, 3858.
[24] I. Morishima, H. Fujii, Y. Shiro, S. Sano, *Inorg. Chem.* **1995**, *34*, 1528.
[25] A. L. Balch, R. Koerner, L. Latos-Grażyński, B. C. Noll, *J. Am. Chem. Soc.* **1996**, *118*, 2760.
[26] H. R. Kalish, L. Latos-Grażyński, A. L. Balch, *J. Am. Chem. Soc.* **2000**, *122*, 12478.
[27] T. N. St. Claire, A. L. Balch, *Inorg. Chem.* **1999**, *38*, 684.
[28] T. Yoshida, M. Noguchi, G. Kikuchi, S. Sano, *J. Biochem.* **1981**, *90*, 125.
[29] A. Wilks, P. R. Ortiz de Montellano, *J. Biol. Chem.* **1993**, *268*, 22357.
[30] Y. Liu, P. Moënne-Loccoz, T. M. Loehr, P. R. Ortiz de Montellano, *J. Biol. Chem.* **1997**, *273*, 6909.
[31] F. A. Walker, "Proton NMR and EPR Spectroscopy of Paramagnetic Metalloporphyrins", in: *The Porphyrin Handbook* (Eds.: K. M. Kadish, K. M. Smith, R. Guilard), Academic Press, New York, **2000**, vol. 5, p. 81.
[32] I. Bertini, C. Luchinat, *Coord. Chem. Rev.* **1996**, *150*, 131.
[33] J. S. Lindsey, in: *Metallopophyrins Catalyzed Oxidations* (Eds.: F. Montanari, L. Casella), Kluwer Academic Publishers, Netherlands **1994**, p. 49.
[34] M. O. Senge, X. Feng, *J. Chem. Soc., Perkin Trans. 1* **2000**, 3615.
[35] B. M. L. Chen, A. Tulinsky, *J. Am. Chem. Soc.* **1972**, *94*, 4144.
[36] M. P. Byrn, C. J. Curtis, S. I. Khan, P. A. Sawin, R. Tsurumi, C. E. Strouse, *J. Am. Chem. Soc.* **1990**, *112*, 1865.
[37] B. Sridevi, S. Jeyaprakash Narayanan, T. K. Chandrashekar, U. Englich, K. Ruhlandt-Senge, *Chem. Eur. J.* **2000**, *6*, 2554.
[38] H. J. Callot, E. Schaeffer, *J. Chem. Res. (S)* **1978**, 51; *J. Chem. Res. (M)* **1978**, 0690.
[39] D. P. Arnold, R. C. Bott, H. Eldridge, F. M. Elms, G. Smith, M. Zojaji, *Aust. J. Chem.* **1997**, *50*, 495.
[40] J. L. Hoard, G. H. Cohen, M. D. Glick, *J. Am. Chem. Soc.* **1967**, *89*, 1992.
[41] W. R. Scheidt, Y. J. Lee, *Struct. Bonding* **1987**, *64*, 1.
[42] J. Wojaczyński, L. Latos-Grażyński, T. Gowiak, *Inorg. Chem.* **1997**, *36*, 6299.
[43] K. Susumu, T. Shimidzu, K. Tanaka, H. Segawa, *Tetrahedron Lett.* **1996**, *37*, 8399.
[44] A. Osuka, H. Shmidzu, *Angew. Chem. Int. Ed. Engl.* **1997**, *36*, 135.
[45] J. Wojaczyński, L. Latos-Grażyński, P. J. Chmielewski, P. Van Calcar, A. L. Balch, *Inorg. Chem.* **1999**, *38*, 3040.
[46] H. Kalish, J. E. Camp, M. Stępień, L. Latos-Grażyński, A. L. Balch, *J. Am. Chem. Soc.* **2001**, *123*, 11719.
[47] R. Bonnett, M. J. Dimsdale, *J. Chem. Soc., Perkin Trans. 1* **1972**, 2540.
[48] A. L. Balch, R. Koerner, L. Latos-Grażyński, J. E. Lewis, T. N. St. Claire, E. P. Zovinka, *Inorg. Chem.* **1997**, *36*, 3892.
[49] S. L. Kessel, D. N. Hendrickson, *Inorg. Chem.* **1980**, *19*, 1883.
[50] A. Osuka, K. Maruyama, *J. Am. Chem. Soc.* **1988**, *110*, 4454.
[51] C. K. Chang, *Adv. Chem. Ser.* **1979**, *173*, 162.
[52] C. A. Hunter, J. K. M. Sanders, *J. Am. Chem. Soc.* **1990**, *112*, 5525.
[53] G. N. La Mar, G. R. Eaton, R. H. Holm, F. A. Walker, *J. Am. Chem. Soc.* **1973**, *95*, 63.
[54] R.-J. Cheng, L. Latos-Grażyński, A. L. Balch, *Inorg. Chem.* **1982**, *21*, 2412.
[55] D. V. Behere, R. Birdy, S. Mitra, *Inorg. Chem.* **1982**, *21*, 386.
[56] J. Wojaczyński, L. Latos-Grażyński, W. Hrycyk, E. Pacholska, K. Rachlewicz, L. Szterenberg, *Inorg. Chem.* **1996**, *35*, 6861.
[57] C. Chachaty, P. J. Rigny, *Chem. Phys.* **1982**, *79*, 203.
[58] J. Lisowski, L. Latos-Grażyński, L. Szterenberg, *Inorg. Chem.* **1992**, *31*, 1933.
[59] R. D. Arasasingham, A. L. Balch, C. R. Cornman, J. S. de Ropp, K. Eguchi, G. N. La Mar, *Inorg. Chem.* **1990**, *29*, 1847.
[60] J. Swift, in: *NMR of Paramagnetic Molecules* (Eds.: G. N. La Mar, W. D. Horrocks, Jr., R. H. Holm), Academic Press, New York **1973**, p. 53.
[61] *XPREP*, version 5.1/NT, Bruker Analytical X-ray Systems, **1997**.

Received November 14, 2001
[I01457]